Electronic supplementary information

A quality-by-design inspired approach to develop PET and PP nanoplastic test materials for use in in vitro and in vivo biological assays

Lukas Wimmer[1,2], My Vanessa Nguyen Hoang[1,2], Jacqueline Schwarzinger[1,2], Vesna Jovanovic[3], Boban Anđelković[4], Tanja Cirkovic Velickovic[3,4], Thomas C. Meisel[5], Tassilo Waniek[6], Christiane Weimann[6], Korinna Altmann[6], Lea Ann Dailey[1*]

[1]Department of Pharmaceutical Sciences, University of Vienna, Vienna, Austria

[2]Center of Excellence for Molecular Food Sciences, Department of Biochemistry, University of Belgrade – Faculty of Chemistry, Belgrade, Serbia

[3]Serbian Academy of Sciences and Arts, Belgrade, Serbia

[4]Department of General and Analytical Chemistry, Montanuniversität Leoben, Leoben, Austria

[5]Bundesanstalt für Materialforschung und -prüfung (BAM), Berlin, Germany

*Corresponding

Tween®80 micelles in DLS

Tween®80 solution (5%, w/w) above the critical micelle concentration (CMC) measured with DLS shows micelles of 7.3 ± 0.15 nm in a volume based size distribution (8.4 ± 0.06 nm intensity based distribution). When larger particles are measured with Tween®80 above the CMC as dispersant, micelles introduce a shift of the Z-Ave even when the micelle peak is not visible in the obtained graph.

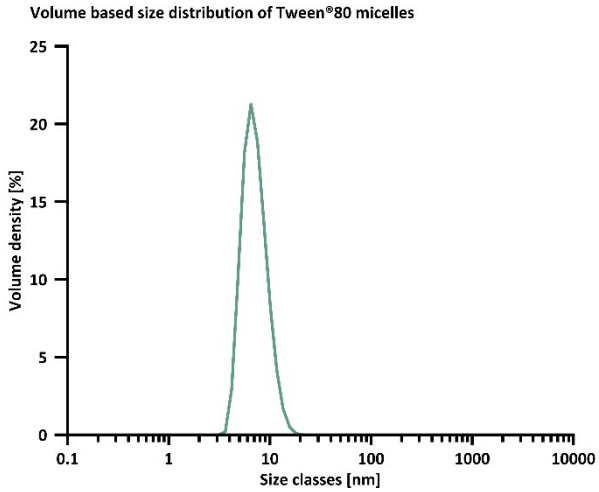

Figure S 1: Volume based size distribution of Tween®80 micelles above the critical micelle concentration.

Variation after production (in ethanol)

After the first production step, the intermediate product (in ethanol) was characterized (Figure S 2). Size distribution analysis revealed that particles < 1 µm were produced with high yields (> 90%) and low variability (< 5%) for both polymer types (Table S 1). The batch-to-batch variation, represented by D_{10} and D_{50}, was higher for PET than for PP but stayed below 13%. In this study, the use of surfactants was limited to quality control (QC) measurements and avoided during production, which led to spontaneous aggregation and a higher degree of variability, especially of the D_{90}. Furthermore, the pronunciation of larger particles in light scattering techniques (higher scattering intensity) also drives the variability in this size range.[1] However, the overlays of the size distribution curves of five

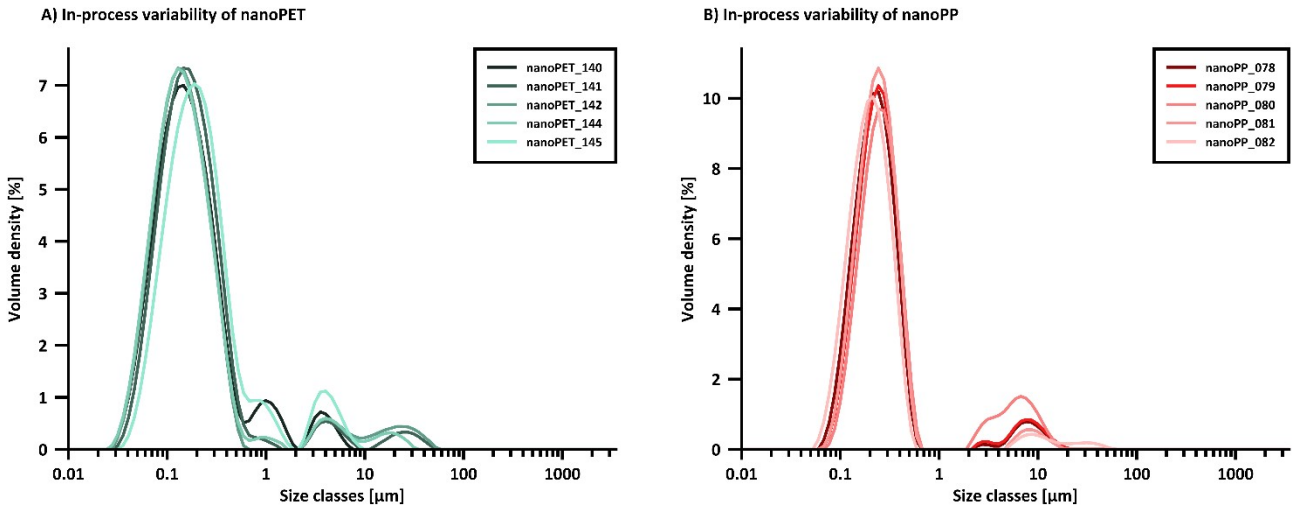

produced batches show excellent similarity, especially in the desired size fraction < 1 µm.

Figure S 2: Comparison of in-process LD particle size distribution curves for five individually produced nanoPET (A) and nanoPP (B) batches dispersed in ethanol using the QC dispersion protocol.

Table S 1: Size distribution data and % < 1 µm of nanoPET and nanoPP batches in-process controls of the intermediate product (in ethanol). Batch-to-batch variability is represented by mean ± SD (RSD%) of n=5 batches per polymer type.

Polymer	Batch in ethanol	D_{10} [µm] (RSD%)	D_{50} [µm] (RSD%)	D_{90} [µm] (RSD%)	% < 1 µm (RSD%)
PET	#140	0.070	0.165	0.589	93.9
	#141	0.077	0.175	0.456	90.7
	#142	0.069	0.157	0.456	92.8
	#144	0.068	0.154	0.439	93.1
	#145	0.089	0.212	0.906	91.5
	Mean	0.0747 ± 0.008 (10.6%)	0.173 ± 0.021 (12.2%)	0.569 ± 0.177 (31.1%)	92.4 ± 1.1 (1.2%)
PP	#078	0.130	0.242	0.461	94.1
	#079	0.141	0.261	0.508	93.0
	#080	0.153	0.288	4.950	85.1
	#081	0.139	0.253	0.450	96.3
	#082	0.115	0.217	0.406	95.7
	Mean	0.136 ± 0.013 (9.3%)	0.252 ± 0.023 (9.2%)	1.36 ± 1.798 (132.7%)	92.8 ± 4.0 (4.3%)

Yields

Table S 2 and Table S 3 list the relative (%) and absolute (mg) yields of all five individually produced batches of nanoPET and nanoPP, respectively. In the last rows, the means and SDs were calculated.

Table S 2: Relative (%) and absolute (mg) yields of produced PET nanoplastics.

Sample	Yield % (absolute mg)
nanoPET_140	92.4 (237.1)
nanoPET_141	86.9 (223.6)
nanoPET_142	90.6 (230.1)
nanoPET_144	95.8 (247.8)
nanoPET_145	87.4 (225.9)
nanoPET_mean	90.6 ± 3.3 (232.9 ± 8.8)

Table S 3: Relative (%) and absolute (mg) yields of produced PP nanoplastics.

Sample	Yield % (absolute in mg)
nanoPP_078	90.4 (153.5)
nanoPP_079	90.3 (151.8)
nanoPP_080	89.4 (149.0)
nanoPP_081	93.5 (156.3)
nanoPP_082	92.6 (152.1)
nanoPP_mean	91.2 ± 1.5 (152.5 ± 2.4)

ATR-FTIR spectra of individual batches

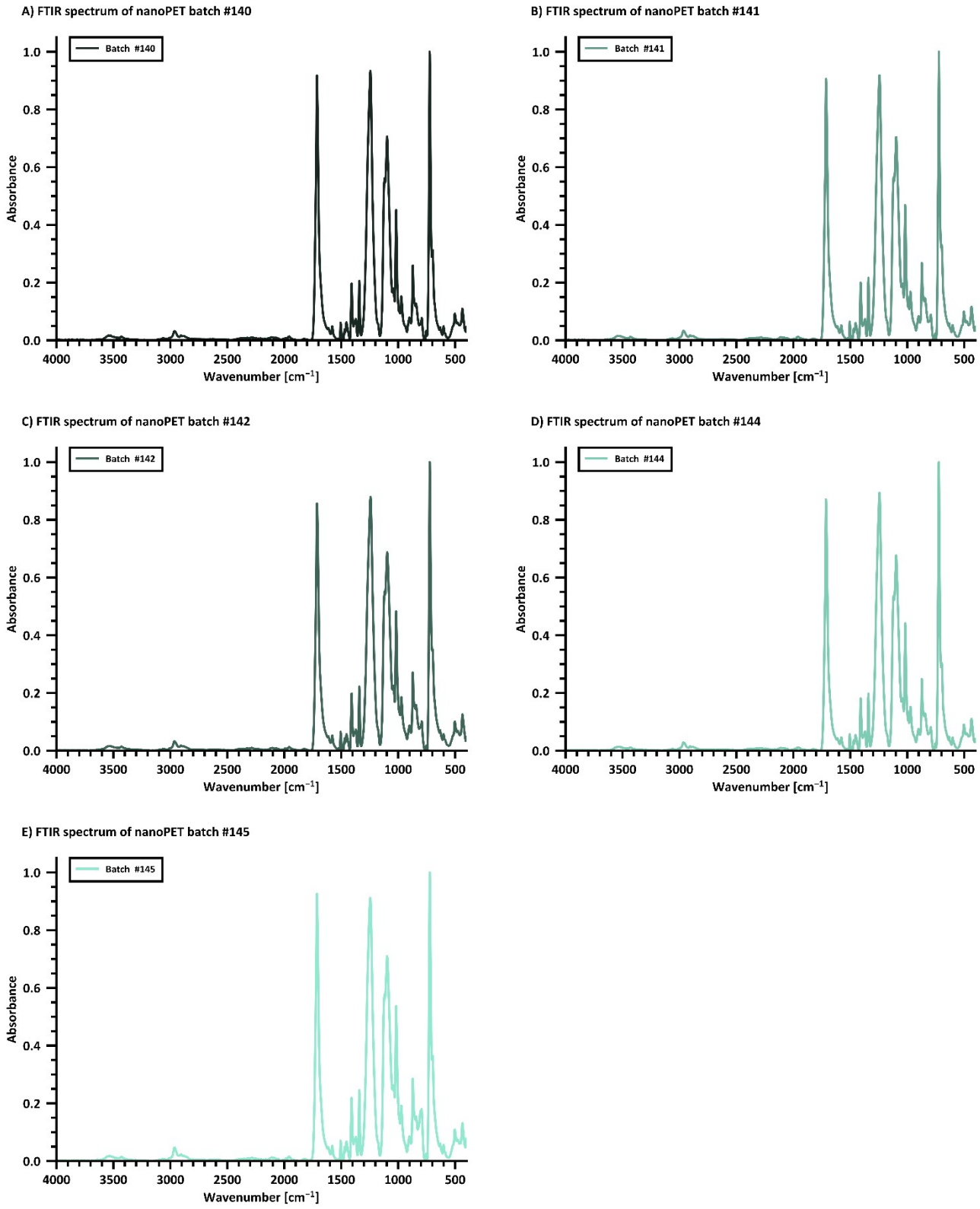

Figure S 3: Individual ATR-FTIR spectra of the five discussed nanoPET batches (#140, #141, #142, #144, #145; A-E).

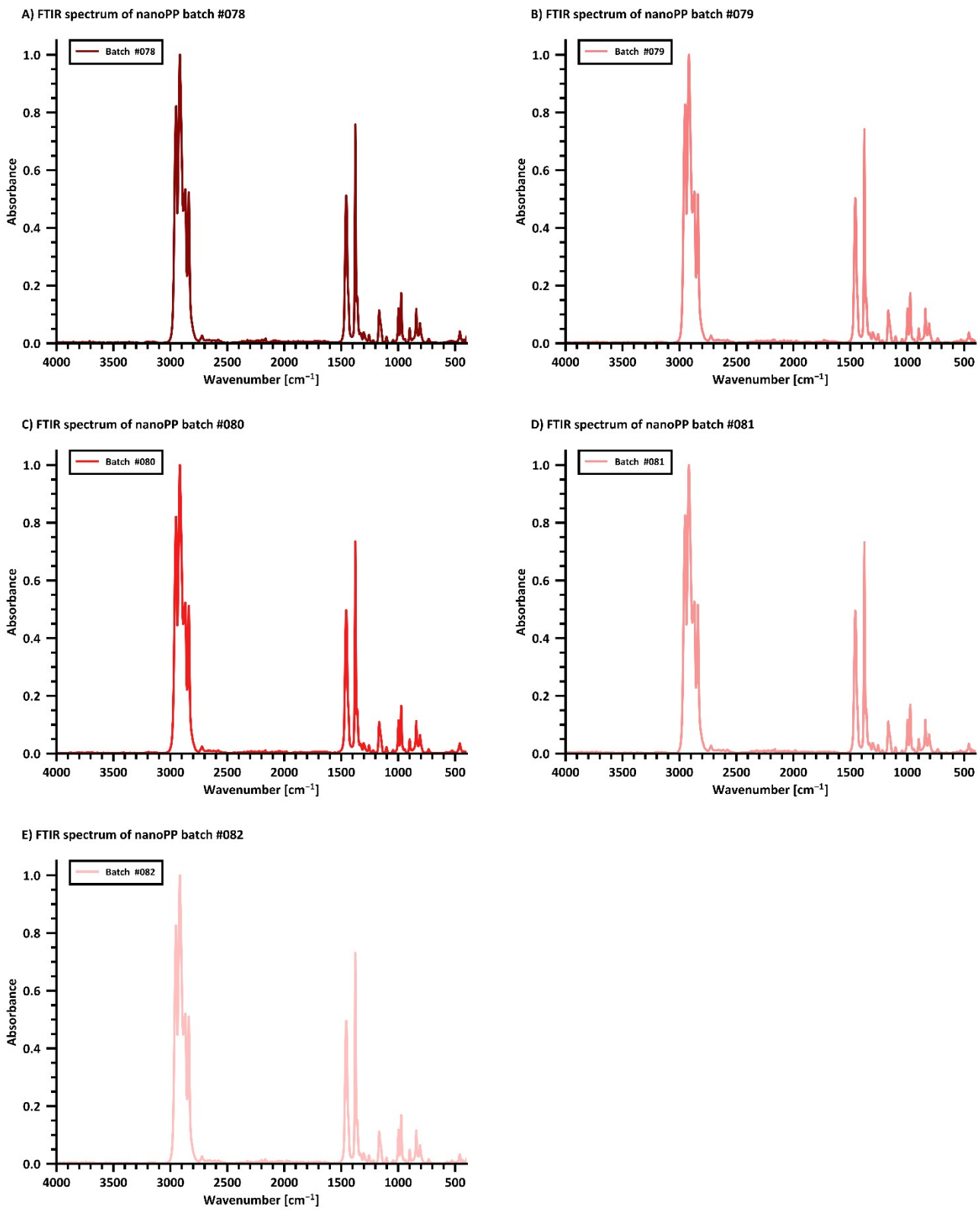

Figure S 4: Individual ATR-FTIR spectra of the five discussed nanoPP batches (#078-#082; A-E).

Intra-batch variability (ethanol vs. glycerol)

To assess the difference between the size distribution of PET nanoplastics before and after the medium exchange from ethanol to glycerol, a one-way ANOVA of the 10^{th}, 50^{th}, and 90^{th} percentile and the % < 1 µm was performed with a CI of 95%. No statistically significant difference between n=5 individually produced batches of nanoPET was detected. In Figure S 5A-E, the distribution curves of all five batches are depicted in ethanol (light colour) and glycerol (dark colour).

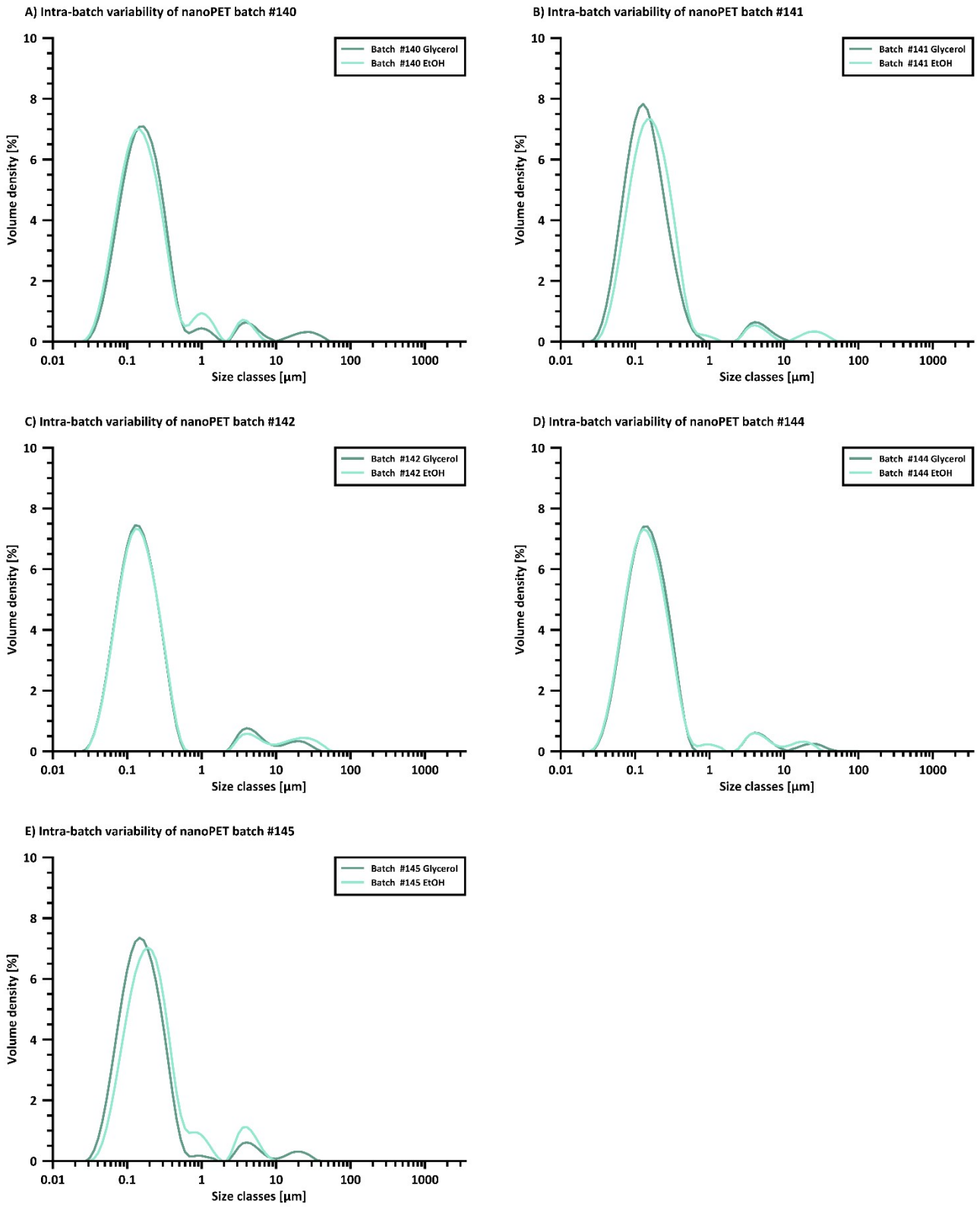

Figure S 5: Intra-batch variability for nanoPET through medium exchange from ethanol to glycerol. A one-way ANOVA of the 10th, 50th, and 90th percentile and % < 1 µm did not show a statistically significant difference between ethanol and glycerol (CI: 95%).

Similarly, the five individually produced batches of nanoPP were assessed and no statistically significant difference between the abovementioned properties could be detected. The size distribution curves of the suspensions in ethanol (light colour) and glycerol (dark colour) are shown in Figure S 6.

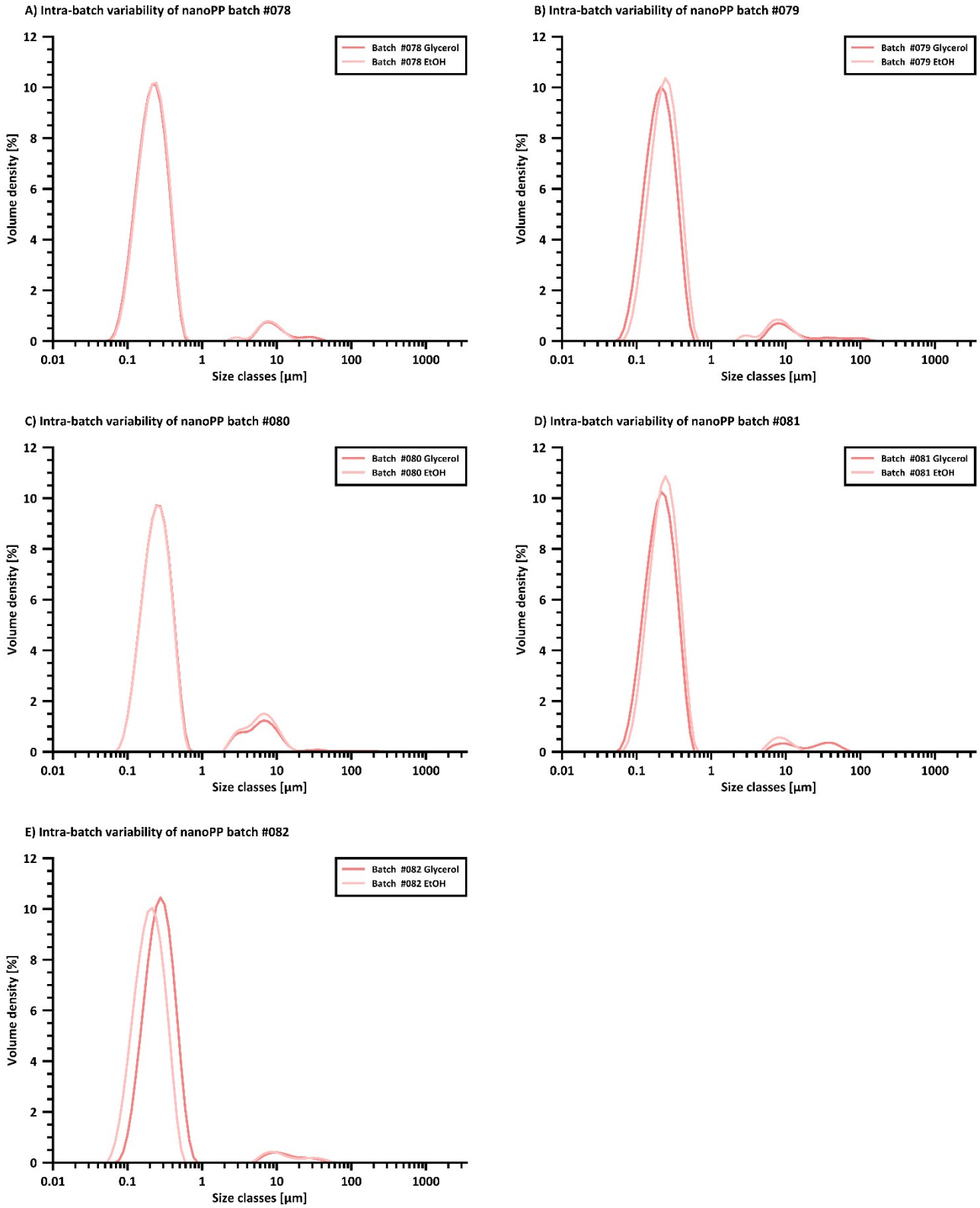

Figure S 6: Intra-batch variability for nanoPP through medium exchange from ethanol to glycerol. A one-way ANOVA of the 10th, 50th, and 90th percentile and % < 1 µm did not show a statistically significant difference between ethanol and glycerol (CI: 95%).

Long-term stability in glycerol

One batch of nanoPET and nanoPP was subject to long-term storage at room temperature under light exclusion for 12 months in their primary package (1 mL glass HPLC vials) in a cardboard box. Samples were drawn immediately after production and after 6, 9, and 12 months. The QC dispersion protocol was applied and the size distribution stability was assessed. The size distribution overlay of nanoPET (Figure S 7A) shows that non-dispersible aggregates form and shift from the 5 µm to the 20 µm region. However, changes of the properties of interest are negligibly small (Table S 4). RSDs of D_{10} and D_{50} are < 15% and therefore considered stable. The high RSD of D_{90} (121.9%) illustrates the formation of non-dispersible aggregates and the % < 1 µm decreased by 1% but stayed high at 89.9%, thus meeting the specification of the TPP.

The nanoPP size distribution curve shows a slight shift after 6 months but stayed unchanged thereafter (Figure S 7B). During 12 months, RSDs of D_{10} and D_{50} stayed below 15%, the % < 1 µm decreased by 6.3% but stayed high at 89.5% and was therefore also considered stable.

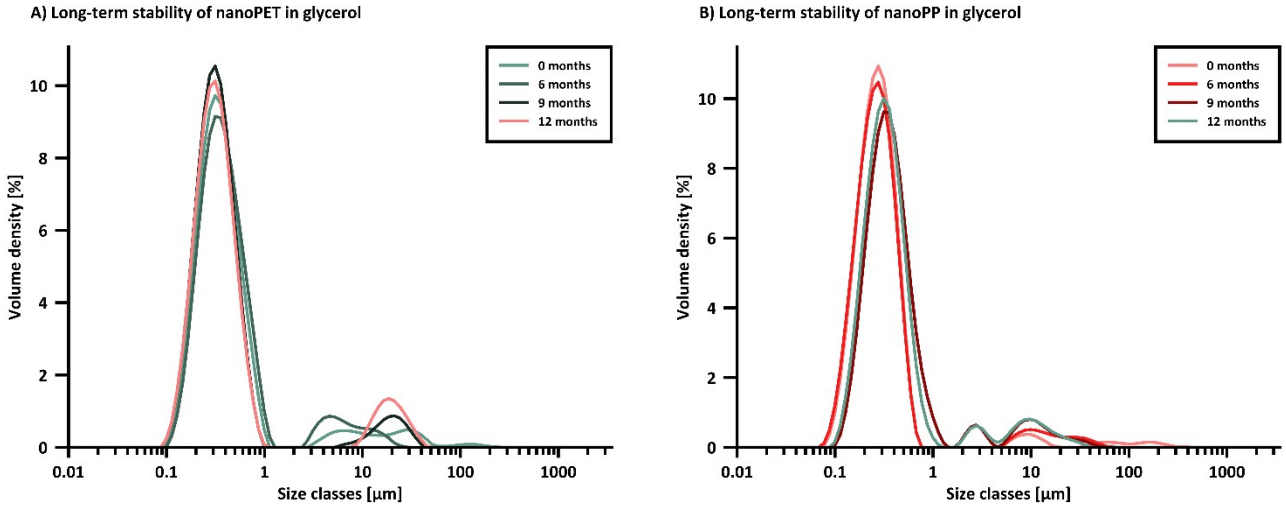

Figure S 7: Size distribution curves of nanoPET (A) and nano PP (B) stored for 0, 6, 9, and 12 months in glycerol. Stocks were dispersed according to the QC dispersion protocol.

Table S 4: Size distribution data and % < 1 µm of nanoPET and nanoPP batches stored in glycerol at RT for 12 months. Variability is represented by mean ± SD (RSD%) of n=4 sampling time points per polymer type.

Polymer	Sampling point	D_{10} [µm] (RSD%)	D_{50} [µm] (RSD%)	D_{90} [µm] (RSD%)	% < 1 µm (RSD%)
PET	0 M	0.202	0.374	0.917	90.9
	6 M	0.211	0.399	1.06	89.5
	9 M	0.191	0.343	0.714	93.1
	12 M	0.191	0.348	9.41	89.9
	Mean	0.199 ± 0.008 (4.2%)	0.366 ± 0.022 (6.1%)	3.03 ± 3.69 (121.9%)	90.8 ± 1.4 (1.5%)
PP	0 M	0.159	0.288	0.517	95.8
	6 M	0.155	0.286	0.546	94.0
	9 M	0.205	0.383	1.300	88.7
	12 M	0.193	0.356	2.160	89.5
	Mean	0.178 ± 0.021 (12.1%)	0.328 ± 0.042 (12.9%)	1.131 ± 0.672 (59.4%)	92.0 ± 3.0 (3.2%)

Further detailed information on corona formation with PET and PP test materials

Studies on the binding capacity and affinity of proteins (specifically BSA) on PP and PET nanoplastics are scarce. We hypothesize, that the difference in re-dispersibility between PET and PP in biologically relevant medium is mainly driven by the different hydrophobicity of the particle surface. Some information is present in the literature. For example, a study using non-modified polystyrene showed that surface hydrophilization *via* aging alters protein absorption and increases the adsorption of hydrophilic proteins from bronchoalveolar lavage fluid[2]. Notably, pristine (more hydrophobic) PS particles showed only minor protein adsorption, while aged (hydrophilized) PS particles were entirely covered[2]. Another study reported a protein binding capacity of PET (0.224 ± 0.005 mg/g)[3]. Further, the binding of BSA on PET microplastics[4] and ovalalbumin to PS and PET microplastics[5] has been studied, with findings that show that the particle size, polymer type and pH all play a role in the complex binding process. Unfortunately, no such experimental data exists for PP nanoplastics. Computational models showed that hydrophobic interactions with hydrophobic and aromatic amino acids are highly relevant in the protein adsorption process for PP[6]. Studies on PP microplastics showed binding of BSA to some extent with stronger binding of a pure protein (BSA) than a protein mixture (yeast extract in this example)[7]. This is in line with our observations, that pure proteins (BSA, OVA) are more effective than mixtures (like FBS).

References

1 M. Kaszuba and M. T. Connah, *Particle & Particle Systems Characterization*, 2006, **23**, 193–196.

2 T. Du, X. Yu, S. Shao, T. Li, S. Xu and L. Wu, *Environ Sci Technol*, 2023, **57**, 3206–3217.

3 Y. Ji, L. Chen, Y. Wang, J. Zhang, Y. Yu, M. Wang, X. Wang, W. Liu, B. Yan, L. Xiao, X. Song, C. Lv and L. Chen, *ACS Nano*, 2024, **18**, 16790–16807.

4 Y. Ji, C. Wang, Y. Wang, L. Fu, M. Man and L. Chen, *Environ Sci Nano*, 2020, **7**, 2313–2324.

5 N Gligorijevic, T Lujic, T Mutic, T Vasovic, MK de Guzman, J Acimovic, D Stanic-Vucinic, T Cirkovic Velickovic, Int J Biol Macromol, 2024, 267, 131564.

6 A. Vismara and A. Gautieri, *Biophys Chem*, 2024, **308**, 107213.

7 M. Schvartz, F. Saudrais, S. Devineau, S. Chédin, F. Jamme, J. Leroy, K. Rakotozandriny, O. Taché, G. Brotons, S. Pin, Y. Boulard and J.-P. Renault, *Langmuir*, 2023, **39**, 4291–4303.